scientific reports

Check for updates

OPEN

Gastrodia protects HT22 cells from damage caused by oxygen glucose deprivation and reperfusion through inhibiting ferroptosis

Dongyue Zhou[1,2], Zhixuan Huang[1,2], Jian Liu[1,2], Jinlong Tan[1,2], Hui Li[1,2,3] & Yangwen Ai[1,2]✉

Gastrodin (Gas) is a key active ingredients of Gastrodia elata Bl., with applications in treating cardiovascular and neurodegenerative conditions. However, the impact of Gas on neuronal damage caused by cerebral ischemia/reperfusion remains uncertain. A cell model of oxygen-glucose deprivation/reoxygenation (OGD/R) was established and the viability and apoptosis of HT22 cells were measured using the CCK-8 assay and TUNEL staining. Different kits detected the levels of LDH, Fe^{2+} and MDA. The levels of ferroptosis-related genes and proteins were evaluated utilizing RT-qPCR and Western blotting. Following OGD/R, there was a decrease in HT22 cell viability and an increase in LDH level and apoptosis rate. Gas (25μM) increased cell viability, decreased LDH, Fe^{2+}, MDA and ACSL4 levels, up-regulated SLC7A11 and GPX4 and ameliorated OGD/R-induced apoptosis ($P < 0.01$). Ferroptosis inducer Erastin (Era, 10μM) successfully induced ferroptosis in HT22 cells, while Gas treatment attenuated the effect of Era. Era further promoted OGD/R-induced damage and ferroptosis in HT22 cells, whereas Gas inhibited the effect of Era. In conclusion, Gas might provide protection against induced HT22 cell injury caused by OGD/R through inhibiting ferroptosis, shows promising potential for clinical treatment of cerebral ischemia/reperfusion.

Keywords Gastrodia, Cerebral ischemia-reperfusion, Ferroptosis, Oxygen-glucose deprivation/Reoxygenation, Neuronal damage

Abbreviations

GPX4	Glutathione peroxidase 4
Gas	Gastrodia
ROS	Reactive oxygen species
Era	Erastin
OGD/R	Oxygen-glucose deprivation/reoxygenation
CCK-8	Cell counting kit-8
SLC7A11	Solute carrier family 7a member 11
ACSL4	Acyl-CoA synthetase long-chain family member 4
LDH	Lactic dehydrogenase

Cerebral infarction is a significant cardiovascular and cerebrovascular disorder that ranks as the foremost contributor to mortality and disability on a global level[1,2]. Cerebral infarction is mainly due to the blockage or interruption of the blood flow to the brain, resulting in ischemia and hypoxia and then necrosis of brain tissues. It is usually of urgent onset and has a high recurrence and disability rate, leading to a serious risk to the patient's life and health[3,4]. The principle of treating acute cerebral infarction is to restore reperfusion to the ischemic area in a timely manner; nevertheless, speedy reperfusion post brain ischemia leads to further harm, i.e., cerebral ischemia/reperfusion injury, which is more severe than cerebral ischemia injury alone[5–7]. Blood reperfusion following ischemia and hypoxia in brain tissue results in the rapid generation of free radicals and the release of numerous inflammatory factors, intracellular calcium overload, and activation of apoptotic genes, which

[1]Jiangxi Province Key Laboratory of Traditional Chinese Medicine Pharmacology, Institute of Traditional Chinese Medicine Health Industry, China Academy of Chinese Medical Sciences, Nanchang 330115, China. [2]Jiangxi Health Industry Institute of Traditional Chinese Medicine, Nanchang 330115, China. [3]Institute of Chinese Materia Medica, China Academy of Chinese Medical Sciences, Beijing 100700, China. ✉email: 13260568664@163.com

accelerates apoptosis of neuronal cells, ultimately leading to neurological dysfunction[8–10]. Therefore, there is an urgent need for effective treatments to avoid cerebral ischemia/reperfusion-induced neuronal injury.

In recent years, ferroptosis has been recognized as a novel form of non-apoptotic cell death, controlled by multiple cellular metabolic pathways such as redox balance, the metabolism of amino acids, lipids, and sugars[11,12]. During ferroptosis in cells, which is usually linked to a large accumulation of free Fe^{2+}, leading to a decrease in the activity of glutathione peroxidase 4 (GPX4) and impacting the metabolism of lipid peroxides, which in turn generates excess reactive oxygen species (ROS)[13,14]. The role of ferroptosis in the progression of ischemic stroke and ischemia/reperfusion injury has been confirmed[15,16]. Cerebral ischemia can induce ferroptosis, and ferroptosis can exacerbate cerebral ischemic injury; therefore, interventions targeting ferroptosis may be an effective way to mitigate cerebral ischemia/reperfusion injury.

Gastrodia elata Bl. is a valuable and traditional Chinese medicine, the origin of which is mainly concentrated in Hubei, Shanxi, Sichuan and Yunnan, China, with neuroprotective, sedative-hypnotic, analgesic and anti-tumor effects[17,18]. Extracted from the dried root mass of Gastrodia elata Bl., Gastrodia (Gas) is an organic compound that plays a significant role as one of the main bioactive components of Gastrodia elata Bl[19]. In recent years, researchers have found that Gas reduces neuroinflammation and is effective in a variety of cardiovascular and neurodegenerative diseases[20–22]. Li et al.[23] showed that Gas inhibits oxidative stress, ameliorates peripheral nerve injury, and promotes peripheral nerve regeneration through the regulation of the miR-497/BDNF axis. Xiao et al.[24] demonstrated that Gas activates the PDE9-cGMP-PKG pathway, improves neurological dysfunction caused by cerebral ischemia, and alleviates neuronal cell damage. Importantly, Jiang et al.[25] discovered that Gas displays strong antioxidant activity and offers defense to neuronal cells from glutamate-induced ferroptosis. However, the mechanism of protective influence of Gas on neuronal ferroptosis due to cerebral ischemia/reperfusion remains unclear.

Therefore, we established an in vitro oxygen-glucose deprivation/reoxygenation (OGD/R) model in this experimental study to investigate how Gas impacts OGD/R-induced ferroptosis in neuronal cells. The aim of this research was to clarify the specific mechanism of action of Gas in alleviating OGD/R injury and to offer a new reference for treating cerebral infarction in clinical settings.

Materials and methods

Cell culture and OGD/R treatment

Mouse hippocampal neuronal cell line (HT22) were obtained from Wuhan Pricella Biotechnology Co., Ltd. (Wuhan, Hubei, China). Sterile culture flasks were used to culture cells in DMEM medium (Gibco, Grand Island, NY, USA) with 10% fetal bovine serum (Gibco) and 1% penicillin/streptomycin (Gibco). The temperature was kept at 37 °C with a 5% CO_2 atmosphere, and the medium was refreshed every 48 h.

Referring to the method of Tassinari et al.[26], HT22 cells were inoculated in 6-well plates and maintained under regular culture conditions for 24 h. Following this, the cells were transferred to a sugar-free and serum-free basal medium and then placed in an anoxic incubator with 95% N_2 and 5% CO_2 for 6 h. The cells were subsequently transferred to normal medium and cultured in a 37 °C environment with 5% CO_2 for 24 h to establish the OGD/R cell model.

Cell counting kit-8 (CCK-8) assay

HT22 cells were collected and seed into 96-well cell culture plates (1.5×10^4 cells/well), and after the cells were wall-approximated, the original medium in the cell culture wells was discarded and replaced with containing different concentrations of Gas (HY-N0115, MedChemExpress, Monmouth Junction, NJ, USA) or ferroptosis inducer Erastin (Era) (HY-15763 MedChemExpress) in culture medium. After 24 h of action, 100 µL CCK-8 reagent (10%, Beyotime, Shanghai, China) was introduced into every well, then cultured in the dark (37 °C, 3 h). Cell viability was ascertained via analyzing the OD_{450} value using a microplate reader (Thermo Fisher Scientific, Waltham, MA, USA).

Determination of lactate dehydrogenase (LDH)

The LDH cytotoxicity assay kit (C0017, Beyotime) was utilized to assess LDH levels in HT22 cells. HT22 cells were collected and inoculated into 96-well cell culture plates (1.5×10^4/well), and once the cell density reached between 70% and 80%, the original medium was swapped with varying concentrations of drug-containing medium. After 24 h of incubation, the 96-well plate was placed in a high-speed centrifuge and centrifuged at 1000 g for 5 min to ensure complete sedimentation of the cells and debris. The liquid above the sediment in each well was extracted, then mixed well with the LDH assay working solution and left to incubate at room temperature for 30 min in a dark environment. Using a microplate reader, the OD_{490} value was determined for each well and the LDH level was then calculated.

TUNEL staining

HT22 cells were exposed to 4% paraformaldehyde (Solarbio, Beijing, China) on slides for 15 min, and subsequently permeabilized with drops of 0.3% Tritonx-100 (Sigma-Aldrich, St. Louis, MO, USA) for 10 min. TUNEL detection solution (C1086, Beyotime) was carefully added and left to incubate in darkness for 1.5 h. The DAPI staining solution (Solarbio) was applied and left to incubate for 10 min in darkness. Fluorescence microscopy was used for observation, and the field of view was randomly selected for photographing.

Determination of MDA level

Western and IP cell lysis solution (P0013, Beyotime) was utilized to lyse HT22 cells at 4 °C. Afterward, the lysate was centrifuged at 12,000 g for 10 min, and the resulting supernatant was then gathered. MDA levels were detected utilizing the MDA ELISA Kit (E-EL-0060, Elabscience Bionovation Inc., Houston, Texas, USA).

Determination of Fe^{2+} level

In accordance with the provided guidelines, the Iron Assay Kit (ab83366, Abcam, Cambridge, MA, USA) was utilized to measure iron levels in HT22 cells. Logarithmic phase HT22 cells were taken, trypsin digested and resuspended in PBS. Mix on ice with iron assay buffer at a 5:1 ratio with the cell suspension. Subsequently, the iron probe was incorporated, mixed gently, and incubated for 60 min. Following the incubation period, the intracellular Fe^{2+} level was assessed by measuring the OD_{593} value utilizing a microplate reader.

RT-qPCR

Trizol reagent (Thermo Fisher Scientific) was utilized to extract RNA from HT22 cells. After that, cDNA was obtained through reverse transcription with the inclusion of AMV reverse transcriptase (TAKARA, Tokyo, Japan). Then, PCR amplification was carried out utilized TB Green® Premix Ex Taq™ II (TAKARA). The internal reference utilized in the analysis was β-actin, and the relative expression of the target gene was determined by the $2^{-\Delta\Delta Ct}$ method.

In this experiment, the primer sequences used are as follows: solute carrier family 7a member 11 (SLC7A11): F: 5'-GGAAGAGGTGAGTGCCTGG-3'; R: 5'-GCCCTGAGGTGTCTGGTTTT-3'. β-actin: F: 5'-TCCTATGG GAGAACGGCAGA-3', R: 5'-TCCTTTGTCCCCTGAGCTTG-3'.

Western blot

RIPA lysate (P0013B, Beyotime) was utilized for lysing cells or tissues to extract proteins, then the BCA kit (P0012, Beyotime) was utilized to determine protein concentrations. The supernatant was taken as protein samples after denaturation. The samples were shifted to PVDF membranes (Invitrogen) and blocked for 3 h following the gel electrophoresis procedure. After rinsing the membrane, placed at a temperature of 4℃ for an overnight incubation with SLC7A11 primary antibody (PA1-16893, 1:1000, Invitrogen), acyl-CoA synthetase long-chain family member 4 (ACSL4) primary antibody (PA5-27137, 1:500, Invitrogen) or GPX4 primary antibody (ab 41787, 1:100, Abcam). On the following day, after being rinsed thrice, the membrane was incubated with goat anti-rabbit secondary antibody IgG (31460, 1:10,000, Invitrogen), exposure after development. Image J software was utilized to obtain the grayscale value of each protein band, with β-actin (MA1-140, 1:5000, Invitrogen) serving as the internal reference.

Statistical analysis

Each experiment was conducted a minimum of three times, and the results were documented as the mean value ± corresponding standard deviation. SPSS 26.0 software (IBM SPSS Statistics 26) was utilized to process and analyze the data statistically. Student's t-test was utilized to evaluate the distinctions between the two groups. ANOVA was applied to make comparisons between sub-multiple groups. Prism software (Graphpad 9.0) was utilized for plotting. $^{*}P < 0.05$, $^{**}P < 0.01$, and $^{***}P < 0.001$ all signifying that there was a significant difference.

Results

Gas ameliorates HT22 cell injury caused by OGD/R

Figure 1A displays the chemical structure of Gas. The impacts of different Gas concentrations (1, 5, 25, and 50 μM) on HT22 cell viability after OGD/R were evaluated using the CCK-8 assay. The findings indicated a marked decrease in HT22 cell viability following OGD/R. Gas at concentrations of 1 μM and 5 μM had no significant impact on cell viability, whereas 25 μM and 50 μM Gas treatments significantly increased cell viability (Fig. 1B). The levels of LDH were notably elevated in HT22 cells following OGD/R. 1 μM and 5 μM of Gas had no significant effect on LDH levels, whereas 25 μM and 50 μM of Gas treatments significantly reduced LDH levels in HT22 cells (Fig. 1C). 25 μM of Gas significantly increased cell viability and decreased LDH levels, so 25 μM of Gas was chosen for subsequent studies. The impact of Gas on apoptosis was assessed using TUNEL staining, revealing a marked increase in the amount of TUNEL-positive cells following OGD/R treatment, while Gas weakened OGD/R-induced apoptosis in HT22 cells (Fig. 1D). These results demonstrated that Gas was able to increase survival rate, and reduce the LDH level and apoptosis rate of HT22 cells, suggesting that Gas could reduce cellular damage caused by OGD/R.

Gas inhibits ferroptosis in HT22 cells induced by OGD/R

In our investigation on the influence of Gas on ferroptosis in HT22 cells, we monitored the variations in Fe^{2+} and MDA levels. Following OGD/R, the levels of Fe^{2+} and MDA in HT22 cells were notably increased, but Gas treatment effectively reduced these levels (Fig. 2A and B). The levels of SLC7A11, a pivotal gene associated with ferroptosis, were evaluated utilizing RT-qPCR and Western blot. The findings indicated a significant decrease in the level of SLC7A11 in HT22 cells following OGD/R, but a significant increase after Gas treatment (Fig. 2C and E). Not only that, the levels of ferroptosis marker proteins ACSL4 and GPX4 in HT22 cells was analyzed using Western blot. Following OGD/R, the findings revealed a notable increase in ACSL4 protein expression and a significant decrease in GPX4 level, while Gas treatment was effective in restoring the abnormal levels of ACSL4 and GPX4 (Fig. 2F and H). The results above demonstrated that OGD/R led to ferroptosis in HT22 cells, and Gas treatment decreased Fe^{2+}, MDA content and ACSL4 protein expression, resulted in increased levels of SLC7A11 and GPX4 proteins, indicating that Gas prevented ferroptosis in HT22 cells induced by OGD/R.

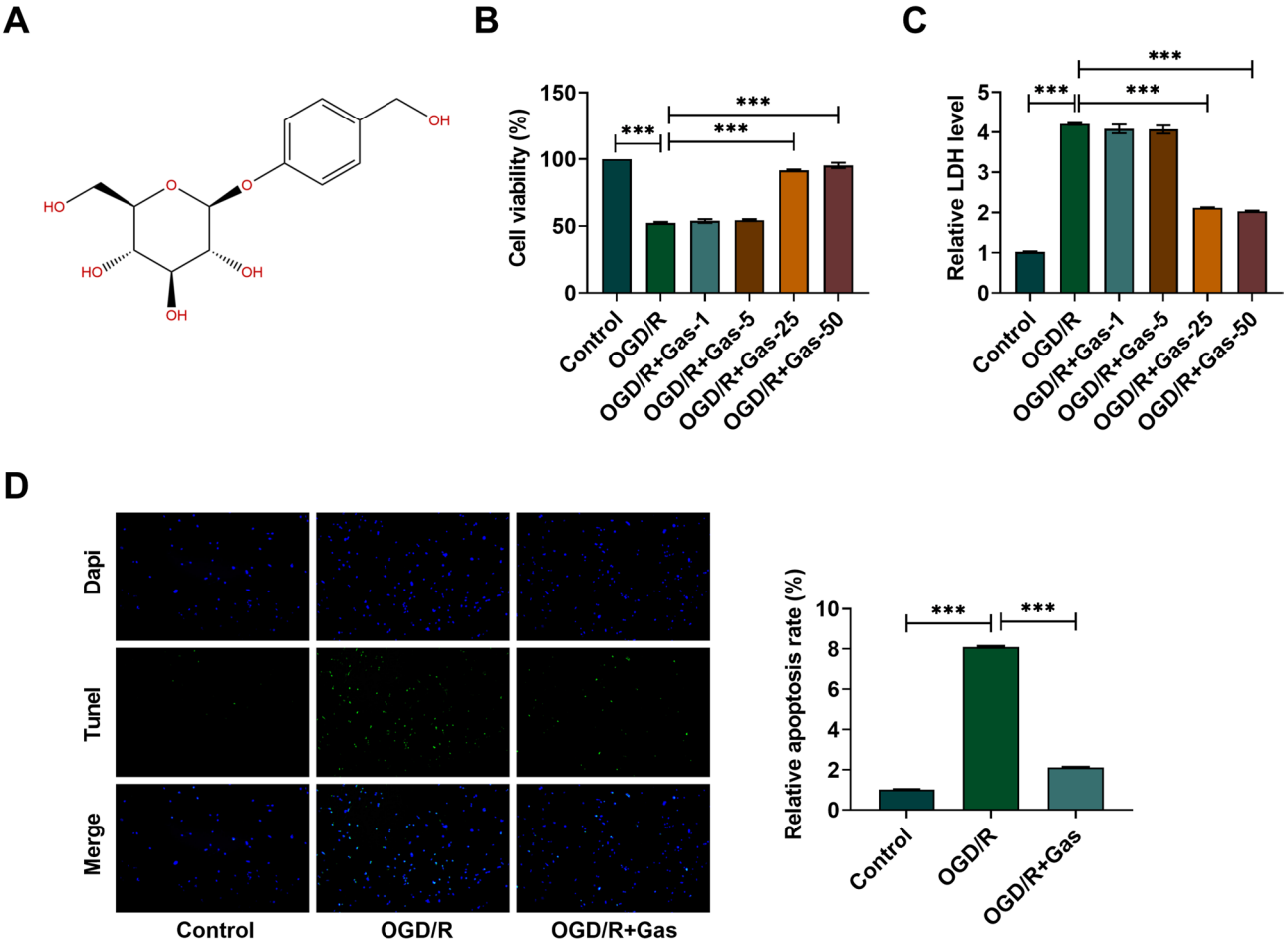

Fig. 1. Gastrodin ameliorates HT22 cell damage induced by oxygen-glucose deprivation/reoxygenation (OGD/R). (**A**) The chemical structural formula of Gas; (**B**) CCK-8 assays of HT22 cell viability; (**C**) LDH levels; (**D**) TUNEL staining of HT22 cell apoptosis rate. All data are presented as mean ± SD ($n = 3$ per group). $^{***}P < 0.001$ indicates statistical significance.

Era induces ferroptosis in HT22 cells

The viability of HT22 cells was determined through CCK-8 assay to investigate the impact of various concentrations of Era. The results indicated that Era (10, 20, and 40 μM) treatments were able to significantly reduce the viability of HT22 cells (Fig. 3A). Consequently, we selected Era at a concentration of 10 μM for further experiments. We found that LDH levels were notably elevated in HT22 cells after Era treatment (Fig. 3B), and Fe^{2+} and MDA contents were also significantly increased (Fig. 3D and E). In addition, following Era treatment, TUNEL staining revealed a marked increase in the amount of TUNEL-positive cells, suggesting that Era induced apoptosis in HT22 cells (Fig. 3C). Not only that, the levels of SLC7A11 mRNA and protein were notably reduced in HT22 cells after Era treatment (Fig. 3F and H). Western blot results showed that Era led to a notable rise in ACSL4 protein level and a marked decline in GPX4 level in HT22 cells (Fig. 3I and K). The above results indicated that Era treatment reduced cell viability, resulting in increased LDH levels and apoptosis, elevated Fe^{2+}, MDA content and ACSL4 protein expression, and reduced the levels of SLC7A11 and GPX4 expression, suggesting that Era could induce ferroptosis successfully in HT22 cells.

Gas hinders ferroptosis in HT22 cells induced by era

Our next step was to explore the influence of Gas on Era-induced ferroptosis in HT22 cells. CCK-8 assay revealed that Era treatment led to a notable reduction in HT22 cell viability, while Gas attenuated the effect of Era (Fig. 4A). Not only that, treatment with Era led to a marked increase in LDH level (Fig. 4B) and Fe^{2+} and MDA contents (Fig. 4D and E) in HT22 cells, Gas treatment reduced the effect of Era. We used TUNEL staining to detect the influence of Gas on Era-induced apoptosis in HT22 cells, and the findings indicated a notable reduction in the amount of TUNEL-positive cells with Gas treatment, suggesting that Gas can inhibit Era-induced apoptosis (Fig. 4C). In addition, following Era treatment, there was a significant drop in SLC7A11 level in HT22 cells, whereas Gas attenuated the effect of Era and up-regulated SLC7A11 expression (Fig. 4F and H). Not only that, ACSL4 protein level was enhanced and GPX4 expression was reduced with Era treatment, while Gas treatment corrected the dysregulated levels of ACSL4 and GPX4 (Fig. 4I and K). These results indicated that Gas increased HT22 cell viability, decreased LDH levels, Fe^{2+} and MDA content, inhibited apoptosis, down-

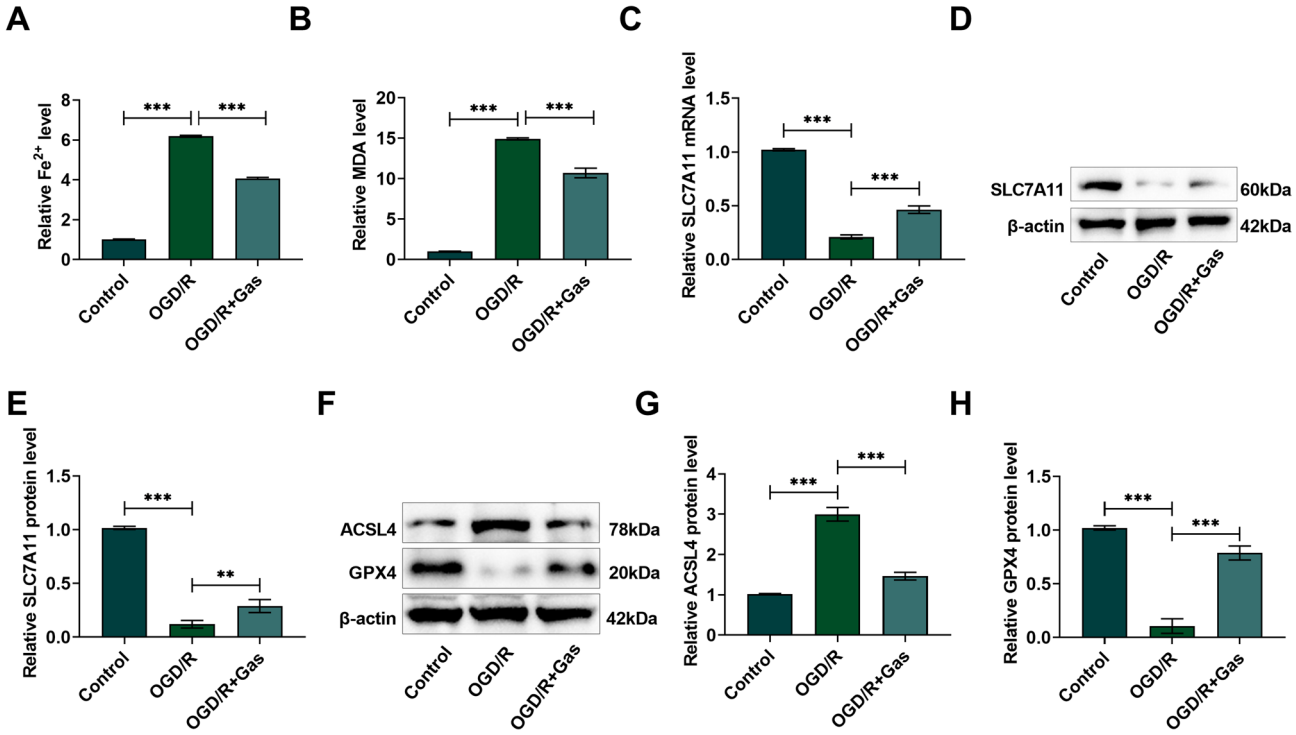

Fig. 2. Gastrodin treatment reduces markers of ferroptosis in HT22 cells subjected to oxygen-glucose deprivation/reoxygenation (OGD/R). (**A**) Fe^{2+} levels; (**B**) MDA levels; (**C**) RT-qPCR analysis of SLC7A11 expression; (**D**–**E**) Western blot analysis of SLC7A11 protein; (**F**–**H**) Western blot analysis of ACSL4 and GPX4 proteins. All data are presented as mean ± SD ($n = 3$ per group). $^{**}P < 0.01$, $^{***}P < 0.001$ indicate statistical significance.

regulated ACSL4 protein expression, up-regulated SLC7A11 and GPX4 level, and inhibited ferroptosis in HT22 cells induced by Era.

Gas protects HT22 cells from injury caused by OGD/R by modulating ferroptosis

We hypothesized that Gas plays an active role in OGD/R-induced HT22 cell damage by regulating ferroptosis. To test our hypothesis, we determined the changes in HT22 cell viability using CCK-8 assay. The findings indicated that Era further decreased HT22 cell viability induced by OGD/R, while Gas treatment significantly increased HT22 cell viability and attenuated the effects of Era and OGD/R (Fig. 5A). In addition, Era further increased LDH levels (Fig. 5B), Fe^{2+} and MDA content (Fig. 5D and E) in OGD/R-induced HT22 cells, while Gas treatment resulted in a decrease in LDH levels, Fe^{2+} and MDA content, which inhibited the effects of Era and OGD/R. According to the TUNEL staining, Era was found to enhance OGD/R-induced apoptosis in HT22 cells, whereas Gas resulted in a notable reduction in apoptosis rate, attenuated the promotional influence of Era and OGD/R on HT22 cell apoptosis (Fig. 5C). Notably, treatment with Era further decreased the level of SLC7A11 in HT22 cells induced by OGD/R, whereas Gas partially reverted this effect (Fig. 5F and H). Treatment with the Era further elevated the level of ACSL4 in HT22 cells following OGD/R, whereas GPX4 expression was further reduced, and Gas treatment attenuated the impacts of Era and OGD/R (Fig. 5I and K). The findings indicated that Era further promoted OGD/R-induced HT22 cell damage and ferroptosis, while Gas inhibited the promotion of cell injury and ferroptosis by Era, suggesting that Gas may offer protection against HT22 cell damage caused by OGD/R by inhibiting ferroptosis.

Discussion

Cerebral ischemia/reperfusion injury is a key element in the pathological process of cerebral infarction, and cerebral ischemia/reperfusion promotes neuronal apoptosis and leads to neurological dysfunction, which has a serious influence on public health[27]. Therefore, the search for novel and efficient drugs to alleviate neuronal cell damage is crucial in improving the prognosis of patients with cerebral infarction. Growing evidence suggests that Gas possesses various pharmacological functions, including anti-inflammatory, antioxidant, anticancer and neuroprotective properties, suggesting its potential in the treatment of various cardiovascular and neurodegenerative diseases[28,29]. Li et al. revealed that Gas can suppress the release of pro-inflammatory cytokines by PI3K/AKT/Nrf2 pathway, leading to the mitigation of OGD/R-induced damage to retinal ganglion cells[30]. In this research, we constructed an OGD/R-induced HT22 cell model to investigate the protective effect of Gas against neuronal injury. We found that Gas treatment increased HT22 cell viability and alleviated OGD/R-induced apoptosis, which is consistent with previous studies.

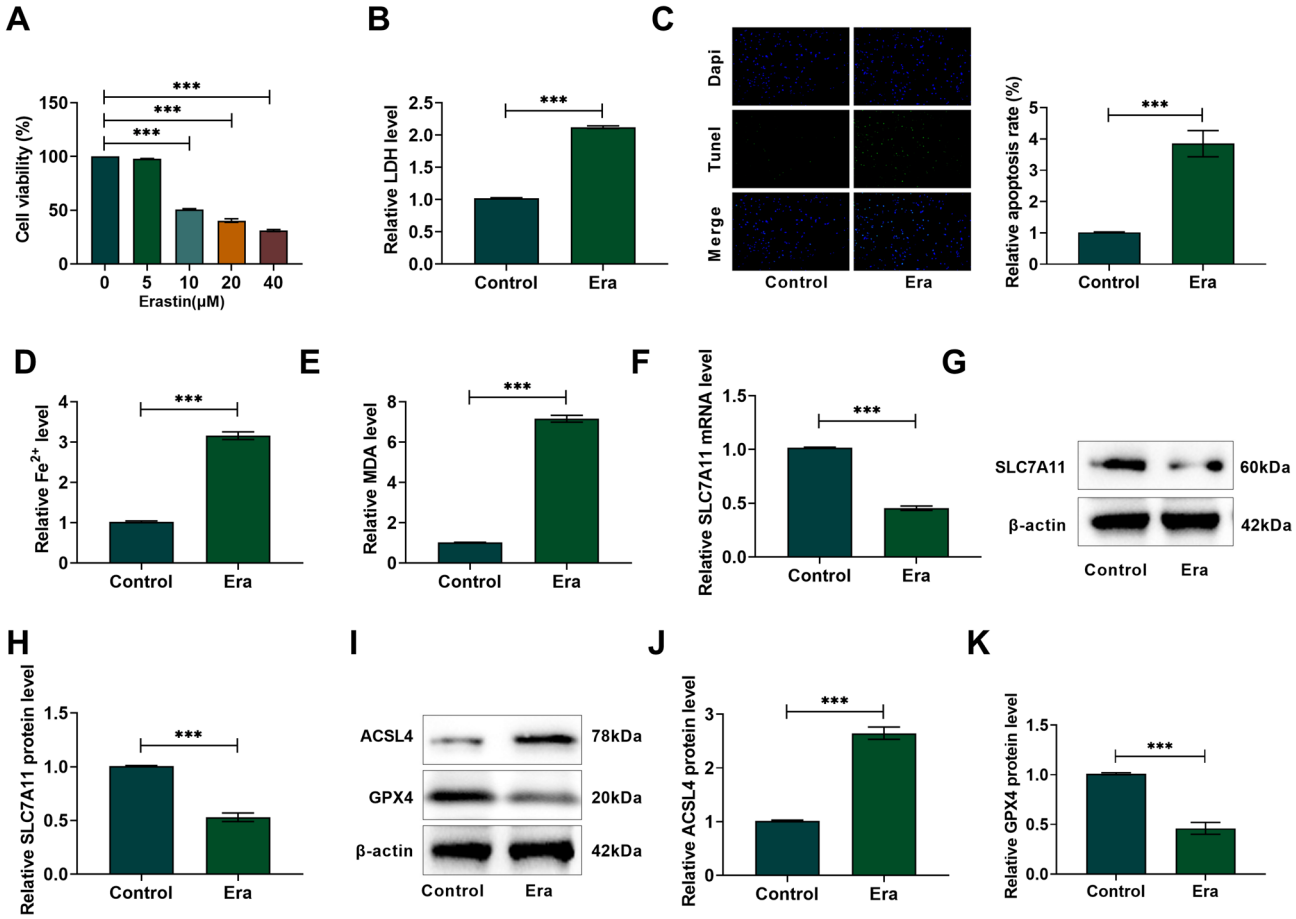

Fig. 3. Erastin can increase markers of ferroptosis in HT22 cells. (**A**) CCK-8 assay of HT22 cell viability; (**B**) LDH levels in HT22 cells; (**C**) TUNEL staining of HT22 cell apoptosis rate; (**D**) Fe^{2+} levels; (**E**) MDA levels; (**F**) RT-qPCR analysis of SLC7A11 expression; (**G**-**H**) Western blot analysis of SLC7A11 protein; (I-K) Western blot analysis of ACSL4 and GPX4 proteins. All data are presented as mean ± SD ($n = 3$ per group). $^{***}P < 0.001$ indicates statistical significance.

To date, the exact cause of cerebral infarction remains unclear, with numerous studies showing a strong connection between ferroptosis and various cardiovascular conditions, including cerebral infarction, ischemic heart disease, myocarditis, and atherosclerosis[31,32]. Ferroptosis involves multiple mechanisms, including Fe^{2+} accumulation, lipid peroxidation, depletion of reduced glutathione, and reduced GPX4 activity[33]. GPX4 is responsible for preventing the formation of lipid peroxides, and MDA is a key product generated during lipid peroxidation[34]. The research by Qiu et al. demonstrated that Gas lowered ROS and MDA levels in human renal tubular epithelial cells and suppressed cisplatin-induced ferroptosis in cells through the SIRT1/FOXO3A/GPX4 pathway[35]. In our research, Gas reduced MDA and LDH levels, inhibited the accumulation of Fe^{2+} levels, and elevated the level of GPX4 protein, indicating that Gas could enhance endogenous antioxidant capacity and thus alleviate OGD/R-induced ferroptosis in cells.

Era is a classical inducer of ferroptosis that mediates iron death through a variety of molecules[36]. SLC7A11, a cystine/glutamate countertransporter protein, is a key protein in the regulation of ferroptosis and inhibits ferroptosis[37]. ACSL4 regulates cellular lipid peroxidation and promotes ferroptosis in cells, and is one of the signature proteins of ferroptosis[38]. We found that Era treatment decreased HT22 cell viability and promoted apoptosis, resulting in a significant increase in LDH levels, Fe^{2+}, MDA content and ACSL4 expression, and down-regulated SLC7A11 and GPX4. Notably, Gas treatment weakened the effect of Era on HT22 cells, indicating a protective role of Gas through the inhibition of ferroptosis. Next, we used Era to intervene in the OGD/R-induced HT22 cell model to investigate if Gas can reduce cellular damage by regulating ferroptosis. Era was found to worsen cell injury and ferroptosis caused by OGD/R, while Gas inhibited the effect of Era and ameliorated cell injury and ferroptosis, confirming that Gas protects HT22 cells from injury caused by OGD/R by inhibiting ferroptosis.

This study first explored the protective properties of Gas in HT22 cell damage induced by OGD/R, as well as the positive impact of Gas on ferroptosis caused by OGD/R. Next, Gas was confirmed to inhibit ferroptosis by constructing an Era-induced ferroptosis cell model. Finally, treatment of OGD/R-induced HT22 cells with Era further confirmed that Gas plays a critical role in neuroprotection by inhibiting ferroptosis (as summary in Fig. 6).

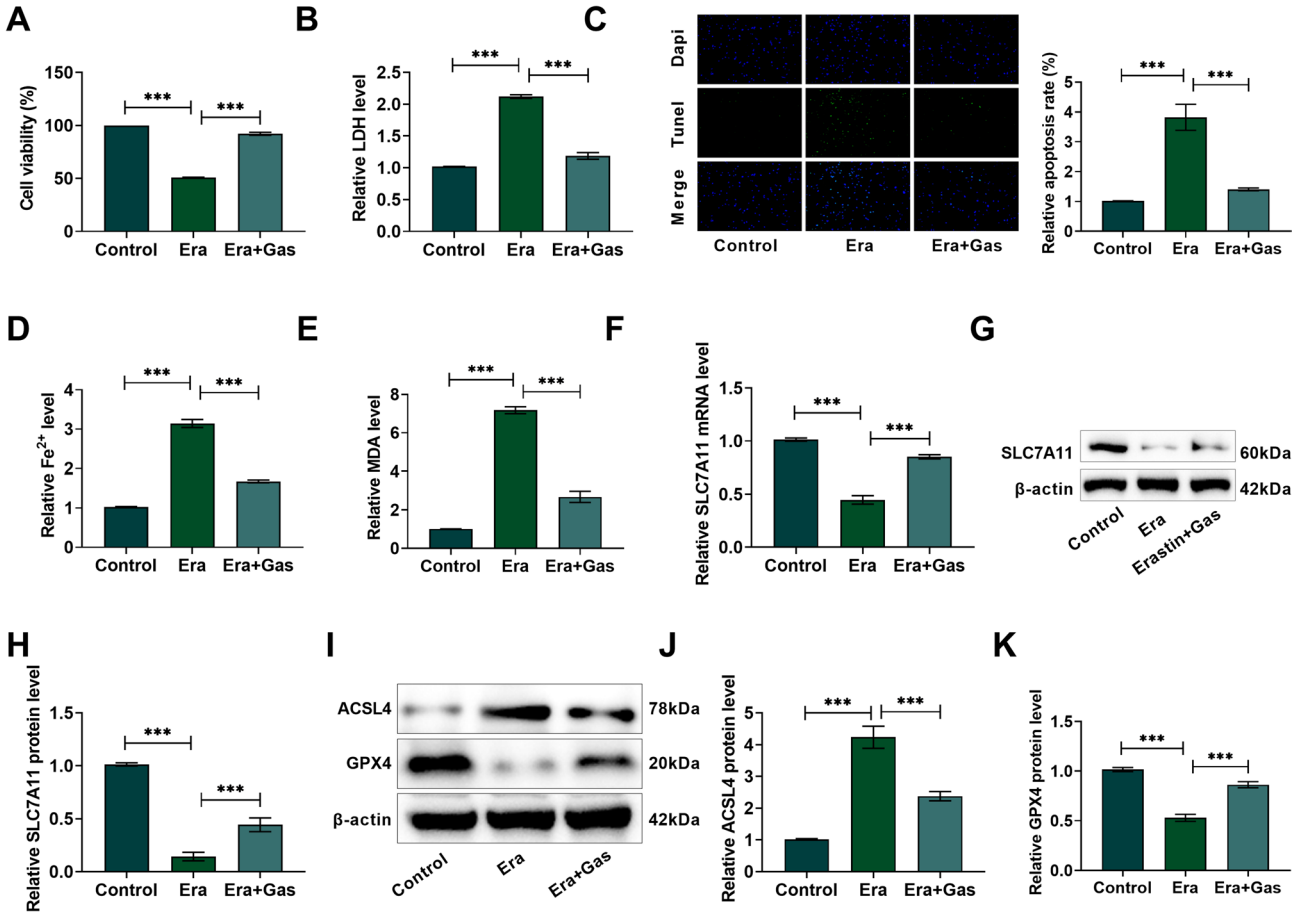

Fig. 4. Gastrodin inhibited ferroptosis in HT22 cells induced by Erastin. (**A**) CCK-8 assay of HT22 cell viability; (**B**) LDH levels in HT22 cells; (**C**) TUNEL staining of HT22 cell apoptosis rate; (**D**) Fe^{2+} levels; (**E**) MDA levels; (**F**) RT-qPCR analysis of SLC7A11 expression; (**G**-**H**) Western blot analysis of SLC7A11 protein; (**I**-**K**) Western blot analysis of ACSL4 and GPX4 proteins. All data are presented as mean ± SD ($n = 3$ per group). $^{***}P < 0.001$ indicates statistical significance.

Conclusion

OGD/R decreased viability and promoted apoptosis of HT22 cells, Era further promoted cell damage and ferroptosis induced by OGD/R, and Gas ameliorated cell injury and ferroptosis caused by OGD/R and Era. Importantly, we identified a novel mechanism by which Gas protects HT22 cells from OGD/R injury by inhibiting ferroptosis. Nonetheless, there are still certain constraints in this study that require further exploration of the safety and effectiveness of Gas in vivo. Based on the results in this paper, we will conduct comprehensive scientific animal experiments to verify its physiological and pharmacological effects more comprehensively. In conclusion, Gas shows promising potential for clinical treatment of cerebral infarction and should be further explored in future research.

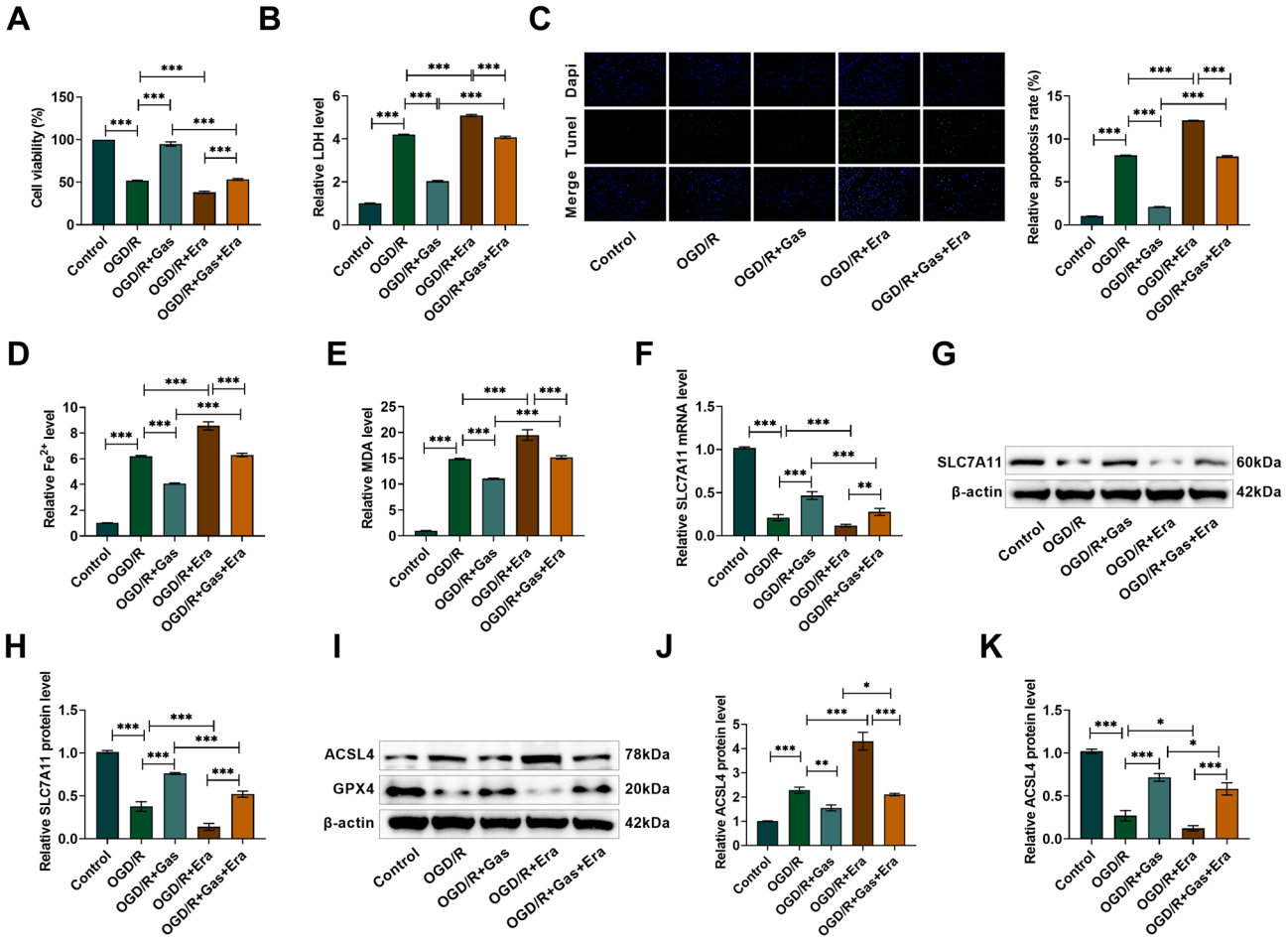

Fig. 5. Gastrodin protects HT22 cells from injury caused by oxygen-glucose deprivation/reoxygenation (OGD/R) through modulating ferroptosis. (**A**) CCK-8 assay of HT22 cell viability; (**B**) LDH levels in HT22 cells; (**C**) TUNEL staining of HT22 cell apoptosis rate; (**D**) Fe^{2+} levels; (**E**) MDA levels; (**F**) RT-qPCR analysis of SLC7A11 expression; (**G**-**H**) Western blot analysis of SLC7A11 protein; (**I**-**K**) Western blot analysis of ACSL4 and GPX4 proteins. All data are presented as mean ± SD ($n = 3$ per group). $^{*}P < 0.05$, $^{**}P < 0.01$, $^{***}P < 0.001$ indicate statistical significance.

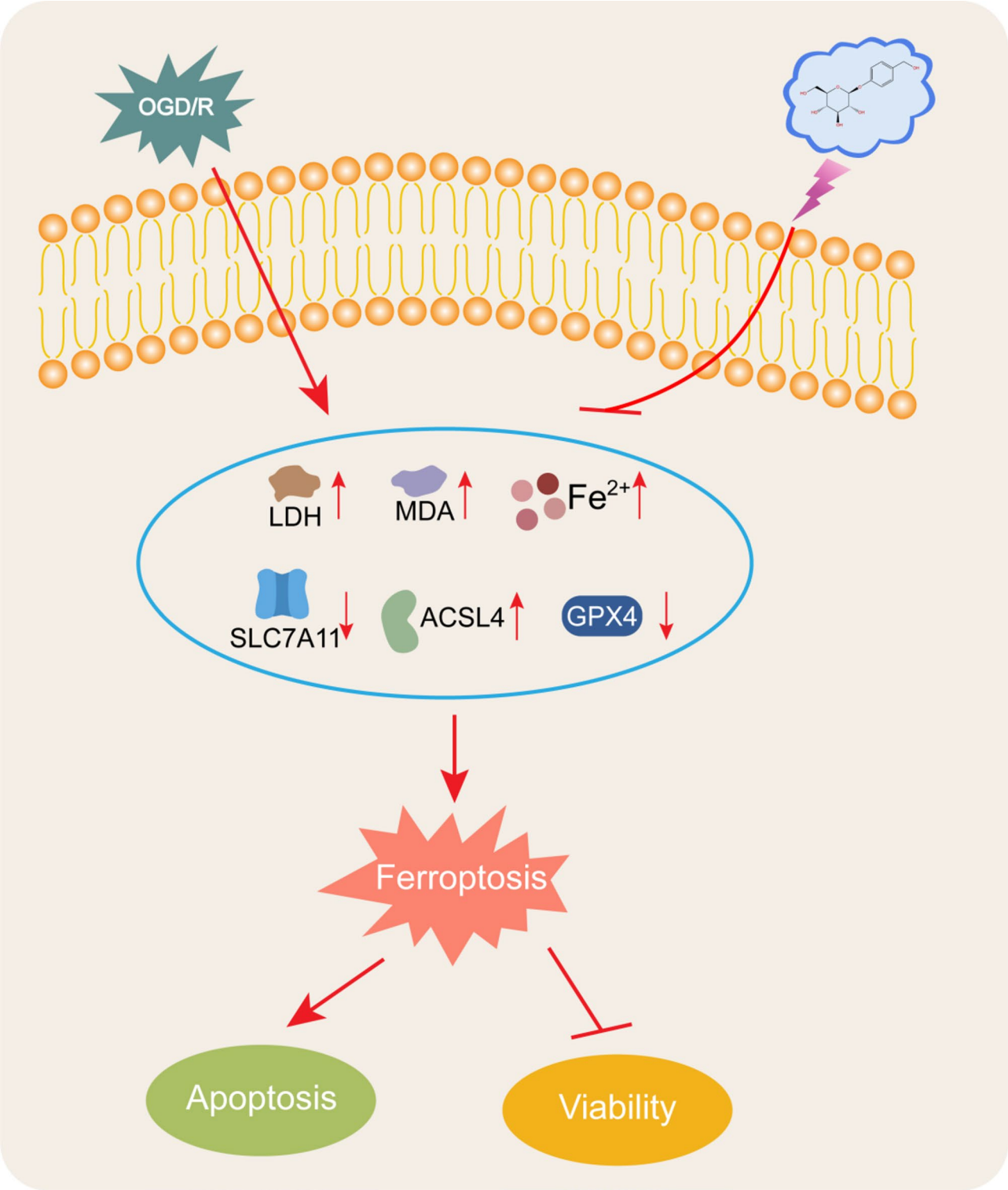

Fig. 6. Diagram of mechanism.

Data availability

Research data are stored in an institutional repository and will be shared with the corresponding author upon reasonable request.

Received: 31 December 2024; Accepted: 20 May 2025
Published online: 27 May 2025

References

1. Yang, K. et al. A systematic review of the research progress of non-coding RNA in neuroinflammation and immune regulation in cerebral infarction/ischemia-reperfusion injury. *Front. Immunol.* **13**, 930171 (2022).
2. Zhao, Y. et al. Neuronal injuries in cerebral infarction and ischemic stroke: from mechanisms to treatment (Review). *Int. J. Mol. Med.*, **49**(2). (2022).
3. Beez, T. et al. Decompressive craniectomy for acute ischemic stroke. *Crit. Care*. **23** (1), 209 (2019).
4. Murphy, S. J. & Werring, D. J. Stroke: causes and clinical features. *Med. (Abingdon)*. **48** (9), 561–566 (2020).
5. Zhang, Q. et al. Cell death mechanisms in cerebral Ischemia-Reperfusion injury. *Neurochem Res.* **47** (12), 3525–3542 (2022).
6. Przykaza, Ł. Understanding the connection between common stroke comorbidities, their associated inflammation, and the course of the cerebral ischemia/reperfusion cascade. *Front. Immunol.* **12**, 782569 (2021).
7. Tuo, Q. Z., Zhang, S. T. & Lei, P. Mechanisms of neuronal cell death in ischemic stroke and their therapeutic implications. *Med. Res. Rev.* **42** (1), 259–305 (2022).
8. Mao, R. et al. Neuronal death mechanisms and therapeutic strategy in ischemic stroke. *Neurosci. Bull.* **38** (10), 1229–1247 (2022).
9. Orellana-Urzúa, S. et al. Pathophysiology of ischemic stroke: role of oxidative stress. *Curr. Pharm. Des.* **26** (34), 4246–4260 (2020).
10. Yıldızhan, K., Güneş, H. & Taskiran, A. Effect of Anakinra and Infliximab on oxidative stress and caspase activation in PTZ-Induced acute seizure in rats. *Eastern J. Med.* **28**, 75–81 (2023).
11. Jiang, X., Stockwell, B. R. & Conrad, M. Ferroptosis: mechanisms, biology and role in disease. *Nat. Rev. Mol. Cell. Biol.* **22** (4), 266–282 (2021).
12. Li, J. et al. Ferroptosis: past, present and future. *Cell. Death Dis.* **11** (2), 88 (2020).
13. Dixon, S. J. & Pratt, D. A. Ferroptosis: A flexible constellation of related biochemical mechanisms. *Mol. Cell.* **83** (7), 1030–1042 (2023).
14. Hadian, K. & Stockwell, B. R. *SnapShot: Ferroptosis Cell.*, **181**(5): 1188–1188e1. (2020).
15. Wu, X. et al. Ferroptosis as a novel therapeutic target for cardiovascular disease. *Theranostics* **11** (7), 3052–3059 (2021).
16. Chen, Y. et al. Ferroptosis: A novel therapeutic target for Ischemia-Reperfusion injury. *Front. Cell. Dev. Biol.* **9**, 688605 (2021).
17. Wu, Y. N. et al. Gastrodia elata BI.:A comprehensive review of its traditional use, botany, phytochemistry, pharmacology, and pharmacokinetics.*Evid. Based Complement Alternat. Med.*, 2023: p. 5606021. (2023).
18. Sun, X. et al. Gastrodia Elata Blume: A review of its mechanisms and functions on cardiovascular systems. *Fitoterapia* **167**, 105511 (2023).
19. Xu, C. B. et al. Gastrodin derivatives from Gastrodia Elata. *Nat. Prod. Bioprospect.* **9** (6), 393–404 (2019).
20. Xie, H. et al. Gastrodia Elata Blume polysaccharides attenuate Vincristine-Evoked neuropathic pain through the Inhibition of neuroinflammation. *Mediators Inflamm.* **2021**, p9965081 (2021).
21. Zhou, H. B. et al. Mechanisms for the biological activity of Gastrodia Elata Blume and its constituents: A comprehensive review on sedative-hypnotic, and antidepressant properties. *Phytomedicine* **123**, 155251 (2024).
22. Gong, M. Q. et al. Traditional uses, phytochemistry, pharmacology, applications, and quality control of Gastrodia Elata Blume: A comprehensive review. *J. Ethnopharmacol.* **319** (Pt 1), 117128 (2024).
23. Yongguang, L. et al. Gastrodin promotes the regeneration of peripheral nerves by regulating miR-497/BDNF axis. *BMC Complement. Med. Ther.* **22** (1), 45 (2022).
24. Xiao, H. et al. Gastrodin promotes hippocampal neurogenesis via PDE9-cGMP-PKG pathway in mice following cerebral ischemia. *Neurochem Int.* **150**, 105171 (2021).
25. Jiang, T. et al. Gastrodin protects against glutamate-induced ferroptosis in HT-22 cells through Nrf2/HO-1 signaling pathway. *Toxicol. Vitro*. **62**, 104715 (2020).
26. Tassinari, I. D. et al. Lactate protects microglia and neurons from oxygen-glucose deprivation/reoxygenation.*Neurochem Res*, (2024).
27. Yoshitomi, T. & Nagasaki, Y. Self-Assembling antioxidants for Ischemia-Reperfusion injuries. *Antioxid. Redox Signal.* **36** (1–3), 70–80 (2022).
28. Su, Z. et al. The processing methods, phytochemistry and Pharmacology of Gastrodia Elata Bl.: A comprehensive review. *J. Ethnopharmacol.* **314**, 116467 (2023).
29. Xiao, G. et al. Review on Pharmacological effects of Gastrodin. *Arch. Pharm. Res.* **46** (9–10), 744–770 (2023).
30. Li, S. et al. Gastrodin protects retinal ganglion cells from ischemic injury by activating phosphatidylinositol 3-kinase/protein kinase B/nuclear factor erythroid 2-related factor 2 (PI3K/AKT/Nrf2) signaling pathway. *Bioengineered* **13** (5), 12625–12636 (2022).
31. Liu, G. et al. Ferroptosis in cardiovascular disease. *Biomed. Pharmacother.* **170**, 116057 (2024).
32. Shaghaghi, Z. et al. Ferroptosis inhibitors as potential new therapeutic targets for cardiovascular disease. *Mini Rev. Med. Chem.* **22** (17), 2271–2286 (2022).
33. Čepelak, I., Dodig, S. & Dodig, D. Ferroptosis: regulated cell death. *Arh Hig Rada Toksikol.* **71** (2), 99–109 (2020).
34. Ursini, F. & Maiorino, M. Lipid peroxidation and ferroptosis: the role of GSH and GPx4. *Free Radic Biol. Med.* **152**, 175–185 (2020).
35. Qiu, C. W. et al. Gastrodin alleviates cisplatin nephrotoxicity by inhibiting ferroptosis via the SIRT1/FOXO3A/GPX4 signaling pathway. *J. Ethnopharmacol.* **319** (Pt 3), 117282 (2024).
36. Zhao, Y. et al. The role of Erastin in ferroptosis and its prospects in Cancer therapy. *Onco Targets Ther.* **13**, 5429–5441 (2020).
37. Koppula, P., Zhuang, L. & Gan, B. Cystine transporter SLC7A11/xCT in cancer: Ferroptosis, nutrient dependency, and cancer therapy. *Protein Cell.* **12** (8), 599–620 (2021).
38. Ding, K. et al. Acyl-CoA synthase ACSL4: An essential target in ferroptosis and fatty acid metabolism. *Chin. Med. J. (Engl).* **136** (21), 2521–2537 (2023).

Acknowledgements

Thanks for the support of the research platform of Institute of Traditional Chinese Medicine Health Industry and the project sponsor.

Author contributions

Conceptualization, Y.A. methodology, D.Z., Z.H. software, J.T., J.L. validation and formal analysis, J.T. and Y.A. investigation, J.T., D.Z., J.L. and H.L. writing—original draft preparation, Y.A. writing—review and editing, D.Z. and Z.H. funding acquisition, Y.A. All authors have read and agreed to the published version of the manuscript.

Funding

This work was supported by the Fundamental Research Funds for the Central Public Welfare Research Institutes (grant number: ZZ17-ND-12, KY-QD20230012).

Declarations

Competing interests
The authors declare no competing interests.

Additional information
Supplementary Information The online version contains supplementary material available at https://doi.org/10.1038/s41598-025-03404-x.

Correspondence and requests for materials should be addressed to Y.A.

Reprints and permissions information is available at www.nature.com/reprints.

Publisher's note Springer Nature remains neutral with regard to jurisdictional claims in published maps and institutional affiliations.